COBEM 2023 27TH INTERNATIONAL CONGRESS OF MECHANICAL ENGINEERING

ABCM Brazilian Society of Mechanical Sciences and Engineering
27th ABCM International Congress of Mechanical Engineering
December 04-08, 2023, Florianópolis-SC, Brazil

Identification of the flow pattern from the experimental pressure signal in horizontal pipes carrying two-phase flows

Daniely Amorim das Neves[1]
Saon Crispim Vieira[2]
Juliana Rangel Cenzi[4]
Aline Souza de Paula[1]
Marcelo Souza Castro[3,4]
Adriano Todorovic Fabro[1]
[1]Department of Mechanical Engineering, University of Brasilia, Brasília-DF, Brazil
[2]PETROBRAS. Santos-SP, Brazil
[3]Center for Petroleum Studies, University of Campinas, Campinas, São Paulo, 13083-970, Brazil
[4]School of Mechanical Engineering, University of Campinas, Campinas-SP, Brazil

Abstract. *Identifying the flow pattern in two-phase systems is extremely important, as the flow pattern is directly related to the pressure gradient, and heat transfer from the mixture, in addition to being relevant in matters of flow assurance. This work proposes an approach for identifying the pattern of two-phase flow in horizontal pipes through noninvasive pressure measurements. The flow patterns are classified dimensionless thresholds based on nonlinear analysis of time series, namely the correlation dimension, Lyapunov, and Hurst exponents. The flow patterns analyzed were: stratified-smooth, stratified-wavy, elongated-bubble, slug and dispersed-bubbles. The results indicate that the system response is chaotic for all flow patterns due to the positive sign of the Lyapunov exponent. It was possible to separate oscillatory flows patterns from non-oscillatory flows patterns using the Hurst exponent. Smooth and wavy stratified patterns were separated from intermittent and dispersed bubbles by the correlation dimension. However, the proposed approach provides a flow pattern classification based on the non-linear flow dynamics of a single non-intrusive pressure measurement.*

Keywords: *Two-phase flow, flow pattern classification, nonlinear series, nonlinear chaos analysis*

1. INTRODUCTION

Multiphase flow is the general term used to refer to any flow of fluid with more than one phase or component. This phenomenon can be found in various industries fields such in the production and transportation of oil-gas in the petrochemical industry, in process catalytic cracking and microreactors in the chemical industry, and in nuclear reactor cooling pumps (Meribout *et al.*, 2020; Yue, 2018; Poullikkas, 2003). Flow patterns are the most important characteristic of multiphase flow systems, the presence of some flow patterns, especially slug flow, can produce excessive vibrations, which can cause piping failures (Ishii and Hibiki, 2011; Miwa *et al.*, 2015). Phase velocities and physical properties of fluids, as well as piping geometry, and orientation, determine the flow patterns (Shoham, 2006). In gas-liquid horizontal systems, the flow patterns can be grouped into three categories: separated phases, intermittent, and dispersed flows. The separated phase flow patterns consist of the parallel flow of components bounded by an interface, such as Stratified-Smooth (SS) and Stratified-Wavy (SW). On the other hand, dispersed flows are characterised by small droplets or bubbles from one component dispersed into the other, called Dispersed-Bubbles (DB). The intermittent flow alternates between the other two patterns in which kinematic waves grow in a nominally stable flow to create a significant phase separation, as Elongated-Bubble (EB) and Slug (SL)(Brennen, 2005).

The identification of different flow patterns is essential due to their influence on pressure gradients and various parameters, including heat transfer coefficients and flow assurance issues. This work aims to identify two-phase flow patterns in horizontal pipes using pressure fluctuation signals in the time domain and nonlinear time series analysis techniques. To achieve this, dimensionless parameters such as correlation dimensions, Lyapunov exponents, and Hurst exponents are employed. This work is structured into five main sections: Section 3presents the experimental apparatus specifications, equipment details, and the test matrix. Section 4discuss the obtained results, generates flow pattern maps, and proposes a methodology for flow pattern identification. Section 5provides the conclusions.

2. Nonlinear Dynamic Classifiers

In this section, the dimensionless parameters Correlation Dimension, Lyapunov exponents, and Hurst exponent are briefly presented. They are subsequently used to form a multi-dimensional map for flow pattern classification.

2.1 Hurst exponent

The Hurst exponent (H), introduced by Hurst in 1951, quantifies the long-term memory of a time series, indicating how much it deviates from a random walk. This measure is particularly useful for understanding the behavior of time series data. The calculation of the Hurst exponent involves a process known as R/S analysis, which was formalized by Mandelbrot in the late 1960s. First, the method considers that a discrete time series $y(n)$ where $n = 1, 2, ..., N$ is divided into k non-overlapping segments y_k of size $T = N/k$. Then, the method continues by calculating the mean value of each sub-period y_k,

$$\overline{y}_k = \frac{1}{T}\sum_{j=1}^{T} y_k(j), k = 1, 2, ..., \frac{N}{T}. \tag{1}$$

n R/S analysis, a discrete time series is divided into non-overlapping segments, and the mean values for each segment are calculated. Next, the accumulated departure from the average for each segment is computed. This information is then used to calculate the R/S values for different segment sizes. These R/S values follow a power law concerning segment size. The slope of this power-law relationship is the Hurst scaling exponent,

$$\left(\frac{\overline{R}}{S}\right)_T \propto bT^H, \tag{2}$$

where b is a constant and H, is the Hurst scaling exponent calculated as the slope of the straight line that best fits the $(R/S)_T$ curve on a log-log plot.

The Hurst exponent has values between 0 and 1, and the time series can be classified into three different categories. First, if $H > 0.5$, the time series has persistent increments, i.e, it is likely that the trend pattern of the previous step will be maintained. Second, if $H < 0.5$, the time series has antipersistent increments, i.e., it is likely that the trend pattern of the previous step is reversed, and they represent an oscillating process. Finally, if $H = 0.5$, then each step is independent of the previous ones, and the increment function, which represents the fractional Gaussian noise, corresponds to white noise.

2.2 Correlation dimension

The Correlation Dimension (CD) is a characteristic measure that can be used to describe the geometry of chaotic attractors in terms of self-similarities. Strange attractors with fractional dimensions are typical of chaotic systems, in other words, non-integer dimensions are assigned to geometric objects that exhibit an unusual kind of self-similarity and that show structures at all length scales. GRASSBERGER1983189 proposed a methodology to calculate the correlation dimension given by,

$$CD(\epsilon) = \frac{1}{N(N-1)}\sum_{i=1}^{N}\sum_{j=i+1}^{N}\Theta(\epsilon - \parallel Y_i - Y_j \parallel), \tag{3}$$

where $\Theta(\epsilon - \parallel y_i - y_j \parallel$ is the Euclidean distance between the vectors Y_i and Y_j. $\Theta(x)$ is the Heaviside function with $\Theta(x) = 1$ for $x > 0$ and $\Theta(x) = 0$ for $x < 0$, where $x = \epsilon - \parallel y_i - y_j \parallel$ and ϵ is the vector norm (i.e. radius of a sphere) centered on Y_i or Y_j, r_{min} and r_{max} were set as the minimum and maximum distances between points, respectively.

2.3 Lyapunov exponent

Lyapunov exponents measure the predictability and sensitivity of the system to changes in its initial conditions. Consider two points in the reconstructed state space, y_{n1} and y_{n2}, associated with a neighbouring and a reference trajectory, respectively, their distances are calculated as $\parallel y_{n1} - y_{n2} \parallel = \eta_0$. After time t, it is expected that the new distance will be equal to $\eta = \eta_0 e^{\lambda t}$, where λ is called the Lyapunov exponent. A positive exponent indicates that the reference and neighbouring trajectories diverge and, consequently, are associated with orbital instability and chaos. A negative exponent implies that the trajectories asymptotically tend to a common fixed point. Finally, a zero exponent means that the trajectories maintain their relative positions, thus associated with the orbital stability of deterministic systems Wolf *et al.* (1985); Rosenstein *et al.* (1993).

The number of exponents of Lyapunov is equal to the number of dimensions of the system, since they describe the expansion or contraction of the orbits for each direction. However, it is the largest Lyapunov exponent that is more interesting, since it can be easily calculated and provides evidence of deterministic chaos in the analysed data. Kantz1994 proposed an algorithm for calculating the largest Lyapunov exponent from the reconstructed state space described by the following equation,

$$S(k) = \frac{1}{N}\sum_{i=1}^{N}\ln\left(\frac{1}{\parallel U_i \parallel}\sum_{i\epsilon U_i}\parallel y_{i+k} - y^*_{i+k} \parallel\right), \tag{4}$$

where U_i is the number of neighbours found around point y_{i+k} and y^*_{i+k} is the reference and neighbourhood point.

3. EXPERIMENTAL SETUP

The experimental tests were conducted at the Experimental Laboratory of Petroleum - LabPetro - of the Center for Energy and Petroleum Studies - CEPETRO - at University of Campinas. A horizontal steel pipe with a 3" internal diameter and 4.5 mm of thickness. Tap water and compressed air were used as working fluids. The liquid density, liquid viscosity, gas viscosity, and superficial tension are equal to 998 kg/m^3, 1 cP, 0.001 cP and 0.07 $N.m$, respectively. The gas density was corrected depending on the line pressure and temperature at the measurement section. As shown in Figure 1 the sensors used were three piezoelectric sensor model 1 PCB 112B21 (P_{re1}, P_{re2} and P_{re3}), seven piezoelectric sensors model 2 PCB 106B50 (P_{re4}, P_{re5}, P_{re6}, P_{re7}, P_{re8}, P_{re9}, P_{re10}). In addition, the time series were stored at an acquisition rate of 25.6 kHz for 600 seconds using a National Instruments (NI) acquisition system. In a section of the workbench, visualisation section was installed, where a high-speed camera (Phanton model VEO 640) was positioned, with a 800 fps rate and a 1600×2560 resolution. The main objective of the use of the camera was to visually identify the flow pattern.

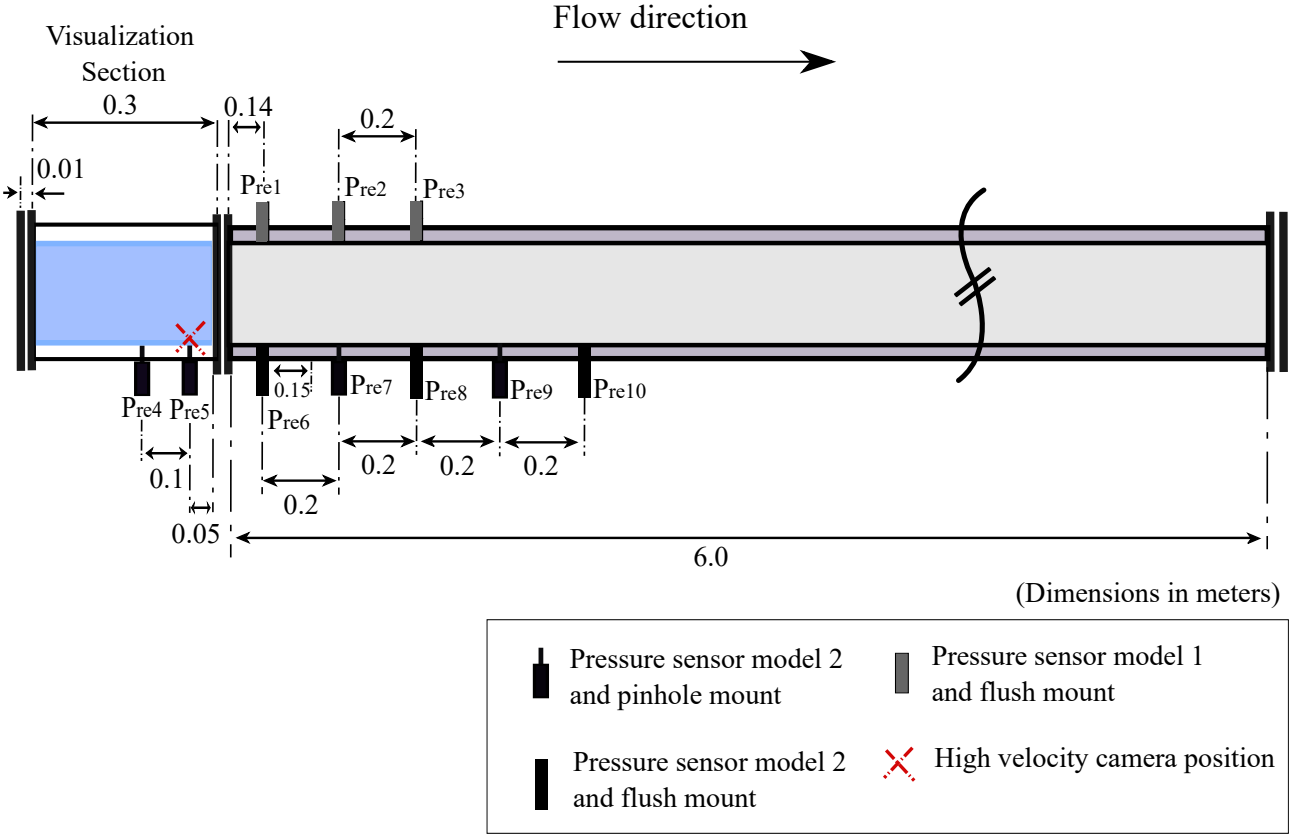

Figure 1. Schematic of the test section on the experimental setup. The positions and distances of the pressure and void fraction sensors are indicated as well as the visualization section where the high-velocity camera was positioned.

A total of 23 experimental points were captured with different superficial gas and liquid velocities(J_{sg} and J_{sl}). The flow pattern was confirmed using the high-speed camera. It was possible to acquire 3 points of the smooth-stratified (SS) pattern, 4 points of the stratified-wavy (SW) pattern, 11 points of the slug (SL) pattern, and 2 points of the dispersed bubbles (DB) pattern.

4. RESULTS AND DISCUSSION

Figure 2 shows the value of h for each point of the test matrix for all pressure sensors. The results are grouped by experimental point and each vertical bar represents a pressure sensor sequentially distributed from P_{re1} to P_{re10}. Note that, the stratified point values are between $1 > h > 0.5$, which means that the series is persistent. As for the intermittent patterns, the values of h are between $0 < h < 0.5$, which corresponds to an anti-persistent series. This is linked to the oscillatory behavior of this pattern varying between the liquid piston and the Taylor bubble, consequently, the exponent value was below 0.2 for most points of the slug pattern. However, observe that for the experimental points P8 and P9, the values of h are a little higher than the other points of the slug pattern, but still below 0.5, in these points, the Taylor bubble is bigger, that is, higher incidence in the stratified region.

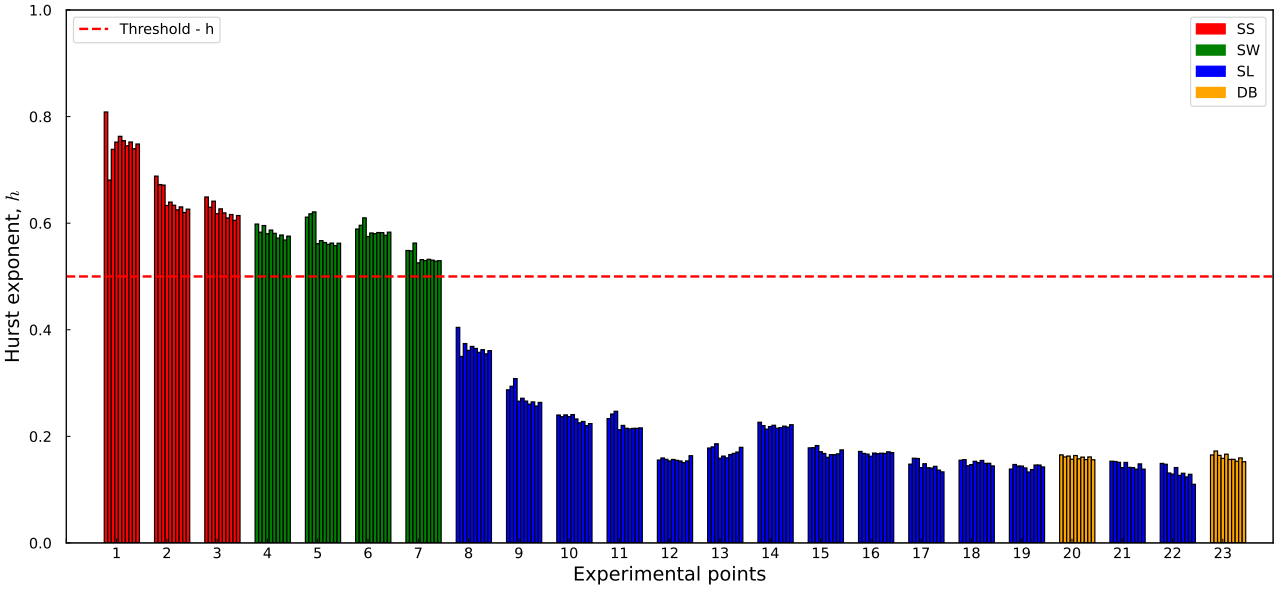

Figure 2. Hurst exponent value (h) calculated from the pressure time series, for all 23 experimental points of the test matrix and sensors. The values are grouped in a set of ten vertical bars, each bar being a sensor, distributed sequentially from P_{re1} to P_{re10}. And each color represents a flow pattern: red for stratified-smooth pattern (SS), green for stratified-wavy (SW), blue for slug (SL), and yellow for dispersed bubbles (DB).

Figure 3 shows the average value of the distances between close trajectories (d_t) of each experimental point calculated by the Lyapunov algorithm, observing that the intermittent patterns present a value of d_t greater than the other patterns. Furthermore, all exponents are positive, indicating that the trajectories of dynamical systems are sensitive to small changes in initial conditions and exponentially diverge from each other over time, which indicates that although the dynamical system is chaotic, it has a very slow divergence rate.

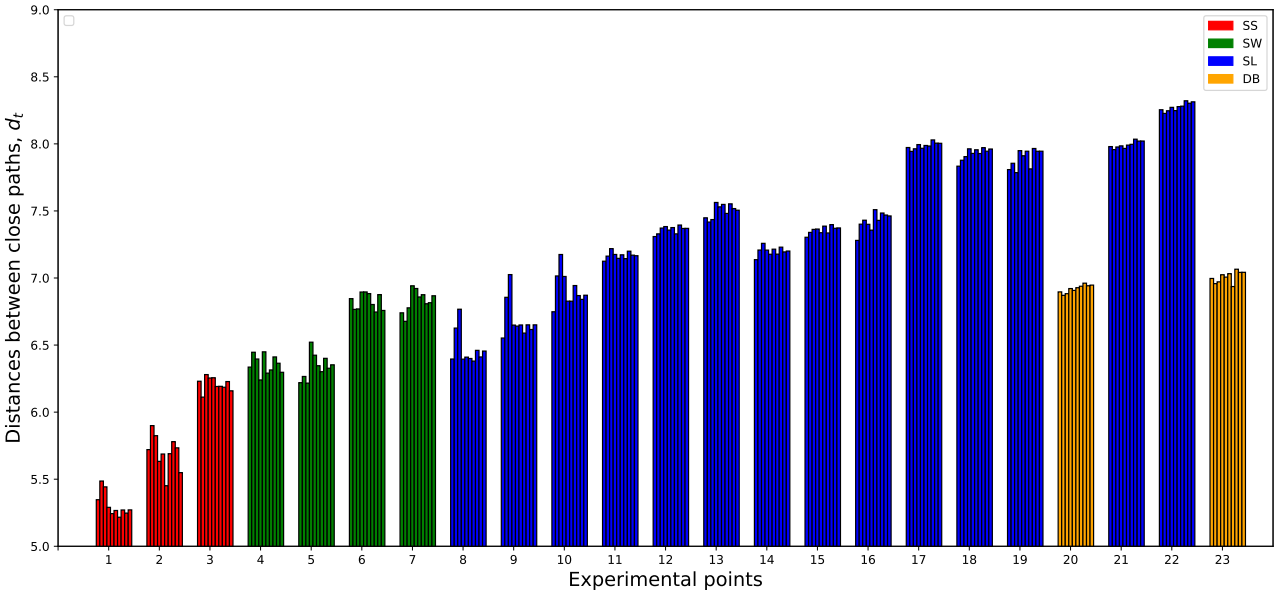

Figure 3. Average values of the distances between close paths (d_t), the values are grouped in a set of ten vertical bars, each bar being a sensor, distributed sequentially from P_{re1} to P_{re10}. And each color represents a flow pattern: red for stratified-smooth pattern (SS), green for stratified-wavy (SW), blue for slug (SL), and yellow for dispersed bubbles (DB).

The correlation dimension coefficient (c) is a measure that describes the geometric complexity of a dynamical system, also known as the fractal correlation dimension or generalized correlation dimension. This is used to estimate the complexity or fractal dimension of a system. Estimation of the correlation dimension coefficient involves reconstructing a phase space from these data. Then, the non-linear dependence between the points in this phase space is measured by means of the correlation between pairs of points at different distances. This correlation is calculated for various distances

and then these values are averaged to obtain the c Grassberger and Procaccia (1983). The delay time (τ) used was estimated using the first local minimum of the mutual information function and the immersion dimension (d_e) estimated by the Broomhead Broomhead and King (1986) method. Thus, Figure 4 presents the estimate of c for all sensors and for all test matrix points. It is possible to observe that the coefficient is less than 4 for the smooth and wavy stratified points. As for the intermittent points and scattered bubbles, the coefficient is higher, indicating a greater complexity in the dynamics. That is, the greater the coefficient, the greater the fractal dimension, indicating greater complexity in the chaotic behavior of the system.

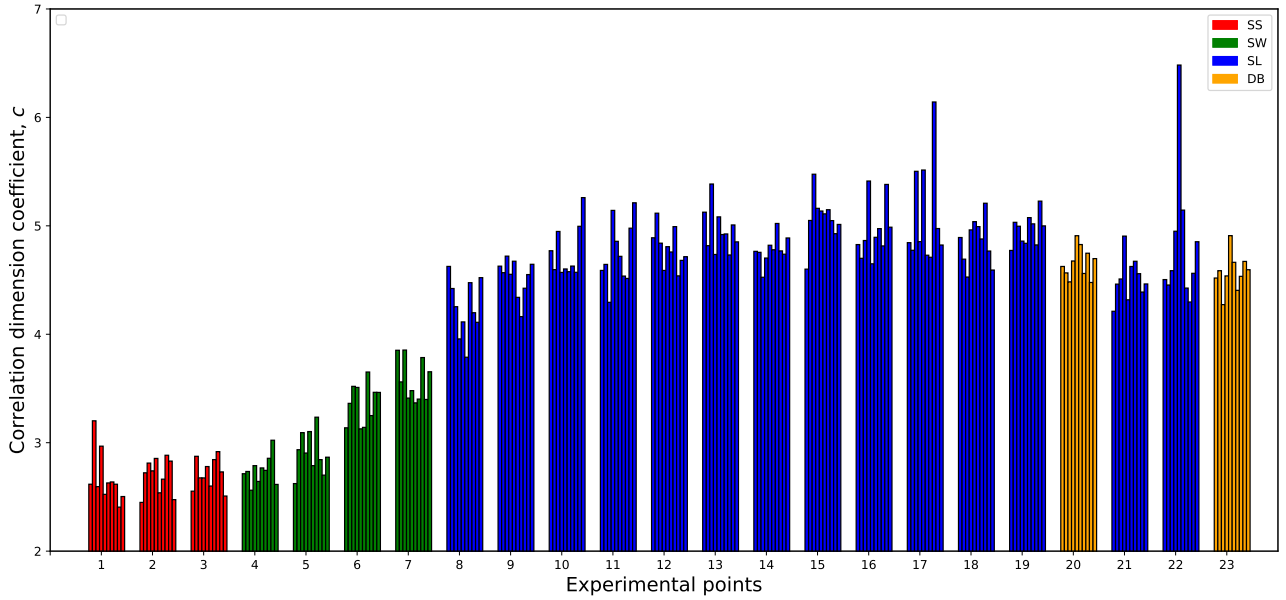

Figure 4. Correlation dimension coefficient (c) calculated from the pressure signals of all 23 experimental points for all sensors. The values are grouped in a set of ten vertical bars, each bar being a sensor, distributed sequentially from P_{re1} to P_{re10}. And each color represents a flow pattern: red for stratified-smooth pattern (SS), green for stratified-wavy (SW), blue for slug (SL), and yellow for dispersed bubbles (DB).

5. CONCLUSIONS

In this work, the flow patterns classification approach was proposed based on dimensionless features of nonlinear time series. The flow patterns reached by the experimental apparatus were Stratified Smooth (SS), Stratified Wavy (SW), Slug (SL) and Dispersed Bubbles (DB). To investigate the dynamics of the system, the invariant indicators of nonlinear systems were calculated, such as Lyapunov exponent, correlation dimension and Hurst exponent. For all points of the matrix, the results yielded a positive Lyapunov exponent, thus indicating a chaotic dynamic. The correlation dimension is intended to determine the dimensions of fractal objects, possibly fractional ones. It was observed that the stratified patterns coefficient of correlation dimension is low when compared to the intermittent patterns since the fractal structures are much smaller in these patterns. The calculated Hurst exponents, which measure the roughness of the experimental series, showed that the stratified patterns presented values smaller than 0.5. On the other hand, the intermittent patterns yielded exponents greater than 0.5, indicating that it captured the dynamics of the oscillatory system at the intermittent flow. Finally, by using such dimensionless parameters, it was able to separate each flow pattern in different regions, which works as a tool for indirect flow pattern identification that can be used in actual industrial systems, as only pressure taps are necessary. Further work will involve investigating the generalisation of this approach to different test benches, with different working fluids and more phases.

6. ACKNOWLEDGEMENTS

We would like to acknowledge PETROBRAS (grant number 2017/00778-2) and ANP for the financial support of this research, the Federal District Research Foundation (FAPDF - Distrito Federal, Brazil) for a post-graduation scholarship of the first author, the Laboratório Experimental de Petróleo (LabPetro) 'Kelsen Valente Serra', at the Center for Energy and Petroleum Studies (CEPETRO), University of Campinas for the experimental facilities, and the Pos-Graduation Program in Mechanical Sciences of the University of Brasilia (UnB)..

7. REFERENCES

The list of references must be inserted as a new section at the end of the manuscript. The first line of each reference must be left-justified. All other lines must be indented 0.5 cm from the left margin. All references listed in the reference list must have been mentioned in the text.

References must be listed in alphabetical order by the last name of the first author. See the following examples:

Brennen, C.E., 2005. *Fundamentals of multiphase flow*, Vol. 53. ISBN 9788578110796.

Broomhead, D.S. and King, G.P., 1986. "Extracting qualitative dynamics from experimental data".

Grassberger, P. and Procaccia, I., 1983. "Measuring the strangeness of strange attractors". *Physica D: Nonlinear Phenomena*, Vol. 9, No. 1, pp. 189–208. ISSN 0167-2789. doi:https://doi.org/10.1016/0167-2789(83)90298-1. URL `https://www.sciencedirect.com/science/article/pii/0167278983902981`.

Ishii, M. and Hibiki, T., 2011. *Thermo-fluid dynamics of two-phase flow*. New York. ISBN 978-1-4419-7985-8. doi:10.1007/978-1-4419-7985-8.

Meribout, M., Azzi, A., Ghendour, N., Kharoua, N., Khezzar, L. and AlHosani, E., 2020. "Multiphase flow meters targeting oil gas industries". *Measurement*, Vol. 165, p. 108111. ISSN 0263-2241. doi:https://doi.org/10.1016/j.measurement.2020.108111. URL `https://www.sciencedirect.com/science/article/pii/S0263224120306497`.

Miwa, S., Mori, M. and Hibiki, T., 2015. "Two-phase flow induced vibration in piping systems". *Progress in Nuclear Energy*, Vol. 78, No. 2015, pp. 270–284. ISSN 01491970. doi:10.1016/j.pnucene.2014.10.003.

Poullikkas, A., 2003. "Effects of two-phase liquid-gas flow on the performance of nuclear reactor cooling pumps". *Progress in Nuclear Energy*, Vol. 42, No. 1, pp. 3–10. ISSN 01491970. doi:10.1016/S0149-1970(03)80002-1.

Rosenstein, M., Collins, J. and De Luca, C., 1993. "A Practical Method for Calculating Largest Lyapunov Exponents from Small Data Sets". *Physica D: Nonlinear Phenomena*, Vol. 65, No. 1-2, pp. 117–134. doi:https://doi.org/10.1016/0167-2789(93)90009-P.

Shoham, O., 2006. *Mechanistic modeling of gas-liquid two-phase flow in pipes*. ISBN 9781555631079.

Wolf, A., Swift, J.B., SWINNEY, H. and Vastano, J., 1985. "Determining Lyapunov exponents from a time series". *Physica D: Nonlinear Phenomena*, Vol. 16, No. 3, pp. 110–123. doi:https://doi.org/10.1016/0167-2789(85)90011-9.

Yue, J., 2018. "Multiphase flow processing in microreactors combined with heterogeneous catalysis for efficient and sustainable chemical synthesis". *Catalysis Today*, Vol. 308, pp. 3–19. ISSN 09205861. doi:10.1016/j.cattod.2017.09.041. URL `http://dx.doi.org/10.1016/j.cattod.2017.09.041`.

8. RESPONSIBILITY NOTICE

The following text, properly adapted to the number of authors, must be included in the last section of the paper:
The author(s) is (are) solely responsible for the printed material included in this paper.